NISTIR 6341

SIMULATING FIRE WHIRLS

Francine Battaglia, Kevin B. McGrattan,
Ronald G. Rehm and Howard R. Baum

Building and Fire Research Laboratory
National Institute of Standards and Technology
Gaithersburg, MD 20899

United States Department of Commerce
Technology Administration
National Institute of Standards and Technology

NISTIR 6341

SIMULATING FIRE WHIRLS

Francine Battaglia, Kevin B. McGrattan,
Ronald G. Rehm and Howard R. Baum

Building and Fire Research Laboratory
National Institute of Standards and Technology
Gaithersburg, MD 20899

July 1999

U.S. Department of Commerce
William M. Daley, *Secretary*
Technology Administration
Gary R. Bachula, *Acting Under Secretary for Technology*
National Institute of Standards and Technology
Raymond G. Kammer, Director

Contents

Simulating fire whirls

Francine Battaglia †, Kevin B McGrattan, Ronald G Rehm and Howard R Baum

National Institute of Standards and Technology, Building and Fire Research Laboratory, 100 Bureau Dr Stop 8640, Gaithersburg, MD 20899-8640

Abstract. A numerical investigation of swirling fire plumes is pursued to understand how swirl alters the plume dynamics and combustion. One example is the 'fire whirl' which is known to arise naturally during forest fires. This buoyancy-driven fire plume entrains ambient fluid as heated gases rise. Vorticity associated with a mechanism such as wind shear can be concentrated by the fire, creating a vortex core along the axis of the plume. The result is a whirling fire. The current approach considers the relationship between buoyancy and swirl using a configuration based on fixing the heat release rate of the fire and imposing circulation. Large eddy methodologies are used in the numerical analyses. Results indicate that the structure of the fire plume is significantly altered when angular momentum is imparted to the ambient fluid. The vertical acceleration induced by buoyancy generates strain fields which stretch out the flames as they wrap around the nominal plume centerline. The whirling fire constricts radially and stretches the plume vertically.

1. Introduction

Fire whirls are a rare but potentially catastrophic form of fire. These swirling buoyant fire plumes are known to increase the danger of naturally occurring or post-disaster fires. Researchers have spent the last four decades investigating these devastating fires [1,2,4-8]. In order for a fire whirl to exist, there must be an organized source of angular momentum to produce the large swirl velocities as air is entrained into the fire plume [1, 2]. These vorticity-driven fires occur over a large range of length and velocity scales, and significantly alter the entrainment and combustion dynamics.

One of the earliest studies to mathematically quantify a fire whirl from experiments was conducted by Emmons and Ying [1]. They reproduced a fire whirl from a pool of acetone centered within a rotating cylindrical screen. The flame was observed to lengthen vertically and tighten radially with increasing screen rotation. The physical

† To whom correspondence should be addressed. Email address: francine@nist.gov

explanation was that the vertical acceleration induced by buoyancy generates strain fields which stretch out the flames as they wrap around the nominal plume centerline. A review by Morton [2] describes the underlying mechanisms which produce and sustain a fire whirl. A mathematical description of a swirling buoyant plume arising from a point source of heat was approached by Thomas and Takhar [3]. Their analyses included cases for which circulation decays to zero outside of the plume or remains a finite constant. While the analysis of these cases showed qualitatively different behavoir, neither would explain the observed plume dynamics found by Emmons and Ying.

The extent of full-scale experimental investigations of fires, in general, are limited by concerns for safety, economy, control and feasibility. Scale modeling is one approach towards investigating fires under more manageable conditions by conducting small-scale experiments [4, 5, 6]. The literature includes reports by Williams [4] which address the importance of scaling mass fires. Soma and Saito [5] have been successful with developing scaling laws to model prototype fire whirls. An extensive review on the progress of experimental investigations in fire spread scenarios has been reported by Hirano and Saito [6].

Recently, an experimental study of swirling fires was pursued by Satoh and Yang [7]. They followed these experiments with a numerical investigation as an additional means to substantiate their observations [8]. The fire took place in a rectangular compartment with vertical asymmetric inlets in order to induce entrainment flow and generate a swirling motion. The model predictions gave quantitatively similar results to that observed in experiments; however, the simulations did not include a combustion model.

Among the studies directed specifically toward fire whirls, there also exists research in the areas of swirling [9, 10] and whirling [11] non-premixed flames. According to Gabler et al. [11], whirling flames differ from swirling flames in that swirl combines both axial and tangential motions of a flow. Whirling flames are described as a rotation produced purely by tangential motion. The studies of swirling flames include details on the effects of varying swirl and jet momentum. The fire whirl experiment [1] was extended by Chigier et al. [9] whereby the liquid pool was replaced with a turbulent jet diffusion flame. The experiments yielded increased flame lengths of the fuel jet with either increasing rotation, increasing flow rates, or both. Tangirala and Driscoll [10] proceeded with studies of a fuel jet surrounded by coaxial swirling air. It was reported that increasing swirl decreased the jet-like flame to a short intense flame, with improved stability, rapid mixing, and increased temperatures. Increasing fuel jet momentum produced a more jet-like flame. At this point, it is important to recognize that jet flames [9, 10, 11] behave differently depending on the application of a rotating flowfield. It would seem that flame lengths tend to decrease when rotation is imparted to the jet, but increase when rotation is imparted to the environment.

To date, fire whirls have not been adequately studied either theoretically or

experimentally, so the impact of swirl on the fluid dynamics and combustion process is not fully understood. Reproducing the characteristics of a fire whirl for any study, whether it be experimental or numerical, is an issue that is addressed in this paper. The swirling motion of a fire has been initiated within a rotating cylindrical screen [1] and vented walls [7, 8]. However, if one is to understand the relationship between buoyancy and angular momentum, it is necessary to identify the magnitude of each attribute. We therefore approach the problem of simulating a fire whirl by imposing circulation into the buoyant plume scenario. In this manner we are able to vary parameters which provides a controlled analysis of the fundamental dynamics of swirling fire plumes.

The phenomenon of a swirling fire can be described physically with critical parameters that control the dynamic mechanisms. To begin, the overall heat release rate determines the strength of the fire. In the absence of any swirl, the fire contains a natural length scale that is a characteristic flame height based on the overall heat release rate and ambient air properties. The length scale together with the gravitational acceleration are used to define scales for velocity and time. The entire problem can be made dimensionless such that the isolated plume depends only on a Reynolds number characterized by an effective kinematic viscosity. The modifications introduced by imposing circulation can now be related to the defined characteristic scales. It is the ratio of the imposed (swirl) circulation to the buoyancy induced circulation that characterizes the relative importance of these mechanisms.

The experiments described above indicate three possible kinds of scenarios. First, the swirl induced circulation is held fixed, and the fire strength is allowed to change [1]. Second, the fire strength is fixed and the geometry determines the strength of the induced swirl [7]. Finally, it is possible to control both the swirl induced circulation and the fire strength using a rotating screen to generate the swirl and a burner (as opposed to a pool fire) to generate buoyancy [9]. This latter scenario can be considered as the "baseline" fire whirl, whose dynamics is the subject of the present paper. Figure 1 is a schematic of the configuration. It is hoped that these constraints will be systematically relaxed in future papers using the methods described below.

The numerical investigations of swirling fire plumes are used to analyze how swirl alters the plume dynamics and combustion. A methodology has been developed to model fires with the use of efficient flow solving techniques and high spatial resolution [12, 13]. An approximate form of the Navier-Stokes equations is solved to calculate the mixing and transport of combustion products. Large scale eddies are directly simulated and sub-grid scale motion is represented with a Smagorinsky model. The fire is prescribed in a manner consistent with a mixture-fraction based approach to combustion [14, 15]. The models and computational methodology have reproduced mean temperature and buoyant velocity correlations for large fire plumes in the absence of circulation [16, 17].

The paper is laid out as follows. Section 2 begins with a description of the problem,

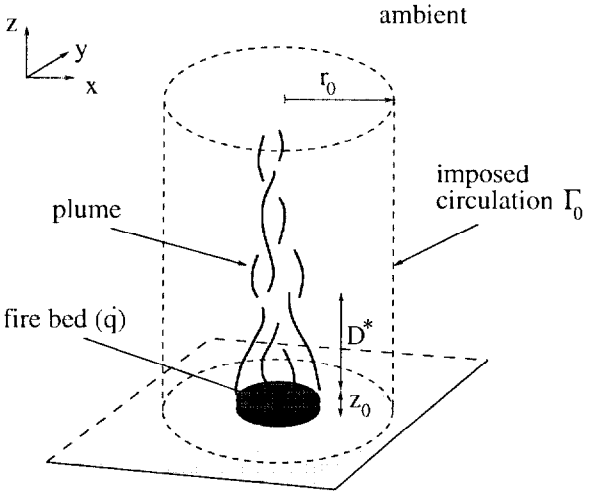

Figure 1. Schematic of a fire plume in ambient conditions under an imposed circulation Γ_0 (e.g., a rotating cylindrical screen). The fire bed is of heat release rate $\dot{q}$ with height z_0 and flame height D^*.

and current large eddy simulation (LES) methodology and combustion model. Section 3 is a presentation and discussion of the LES results for a fire plume in ambient conditions with and without swirl. The discussion begins with a comparison of non-swirling fires and well-established plume correlations. Both non-swirling and swirling plumes are then contrasted to highlight basic physical differences. An important contribution of this paper is the presentation of temperature fields, swirl velocity characteristics, and heat release rate trends with increasing circulation. The summary will address the advantages and limitations of the simulations to establish goals of future work.

2. Methodology

2.1. Hydrodynamic model

The fire plume is a three-dimensional, transient, buoyant flow that can be modeled by the motion of a thermally expandable ideal gas [12]. The Navier-Stokes equations are solved for such a fluid driven by a prescribed heat source, where

$$\frac{\partial \rho}{\partial t} + \nabla \cdot \rho \mathbf{u} = 0 \tag{1}$$

$$\frac{\partial \rho Y_i}{\partial t} + \nabla \cdot \rho Y_i \mathbf{u} = \nabla \cdot \rho D_i \nabla Y_i + \dot{W}_i \tag{2}$$

$$\rho \left(\frac{\partial \mathbf{u}}{\partial t} + \mathbf{u} \cdot \nabla \mathbf{u} \right) + \nabla p - \rho \mathbf{g} = \nabla \cdot \boldsymbol{\tau} \tag{3}$$

$$\frac{\partial \rho h}{\partial t} + \nabla \cdot \rho h \mathbf{u} - \frac{dp_0}{dt} = \dot{q}''' + \nabla \cdot \left(k \nabla T + \sum \rho h_i D_i \nabla Y_i + \dot{q}_R \right) \tag{4}$$

$$p_0(t) = \rho T \mathcal{R} \sum (Y_i / M_i) \tag{5}$$

The fluid variables are density ρ, velocity $\mathbf{u}$, mass fraction of ith species Y_i, mass diffusivity of ith species D_i, production rate of ith species $\dot{W}_i$, pressure p, gravity $\mathbf{g}$, viscous stress tensor $\boldsymbol{\tau}$, enthalpy h, volumetric heat release rate $\dot{q}'''$, thermal conductivity k, temperature T, radiant energy flux $\dot{q}_R$, universal gas constant $\mathcal{R}$, and molecular weight of ith species M_i.

The pressure is decomposed into three components, a background (average) pressure $p_0(t)$, a hydrostatic contribution $-\rho_0 g z$, and a perturbation to the hydrostatic $\tilde{p}(\mathbf{x}, t)$. The subscript 0 is a reference value of density, and z is the vertical coordinate. Equations (4) and (5) are modified using the background pressure p_0 which depends on time t only. In this manner, high-frequency acoustic oscillations are eliminated while large temperature and density variations typically found in fires are retained. The resulting equations are referred to as weakly compressible and are valid for low Mach number flows [12].

A further assumption is that the constant pressure specific heat of the ith species $c_{p,i}$ is independent of temperature. Therefore, the enthalpy is written as

$$h = \sum h_i Y_i = T \sum c_{p,i} Y_i$$

Combining the conservation equations for mass (1), energy (4) and state (5) results in an expression for the divergence of the flow $\nabla \cdot \mathbf{u}$

$$p_0(t) \nabla \cdot \mathbf{u} + \frac{1}{\gamma} \frac{dp_0}{dt} = \frac{\gamma - 1}{\gamma} \left[\dot{q}''' + \nabla \cdot \left(k \nabla T + \sum \rho h_i D_i \nabla Y_i + \dot{q}_R \right) \right] \tag{6}$$

The term $\nabla \cdot \mathbf{u}$ is an important quantity that is later exploited in the numerical solution. Equation (6) is integrated over the entire domain for pressure p_0 and is used as a consistency condition.

The momentum equation (3) is simplified by subtracting off the hydrostatic pressure gradient, and then dividing by the density to obtain

$$\frac{\partial \mathbf{u}}{\partial t} + \frac{1}{2} \nabla |\mathbf{u}|^2 - \mathbf{u} \times \boldsymbol{\omega} + \frac{1}{\rho_0} \nabla \tilde{p} = \frac{1}{\rho} \left((\rho - \rho_0) \mathbf{g} + \nabla \cdot \boldsymbol{\tau} \right)$$

where $\boldsymbol{\omega}$ is the vorticity. The head $\mathcal{H}$ is introduced, where

$$\nabla \mathcal{H} \equiv \frac{1}{2} \nabla |\mathbf{u}|^2 + \frac{1}{\rho_0} \nabla \tilde{p}$$

The final form of the momentum equation is

$$\frac{\partial \mathbf{u}}{\partial t} - \mathbf{u} \times \boldsymbol{\omega} + \nabla \mathcal{H} = \frac{1}{\rho} \left((\rho - \rho_0) \mathbf{g} + \nabla \cdot \boldsymbol{\tau} \right) \tag{7}$$

The quantity $1/\rho_0$ implies that the vorticity generation induced by buoyancy is much more important than that due to baroclinic effects, *i.e.* the non-alignment of the pressure and density gradients.

The equations presented thus far can be solved directly to obtain a solution to the problem of a buoyant fire plume. The difficulty arises in that the length and time scales associated with the fluid dynamics and combustion vary over orders of magnitude. In order to calculate the dynamics of the problem, models for τ and $\dot{q}'''$ are necessary. The goal is to capture mixing on scales where the eddy viscosity is effective which generally requires a very fine grid to resolve the scales. An alternative approach is to use an elaborate sub-grid scale description. One representation of the dynamic viscosity is based on the analysis of Smagorinsky [18] where the sub-grid scale Reynolds stress tensor is given by

$$\tau_{ij} = \mu \left(\frac{\partial u_i}{\partial x_j} + \frac{\partial u_j}{\partial x_i} - \delta_{ij} \frac{2}{3} \frac{\partial u_k}{\partial x_k} \right) ; \qquad \mu = \rho \left(C_s \, \Delta \right)^2 |S|$$

where C_s is an empirical constant, Δ is a length on the order of the grid cell size, and

$$|S|^2 = 2 \left(\frac{\partial u}{\partial x} \right)^2 + 2 \left(\frac{\partial v}{\partial y} \right)^2 + 2 \left(\frac{\partial w}{\partial z} \right)^2 + \left(\frac{\partial u}{\partial y} + \frac{\partial v}{\partial x} \right)^2 + \left(\frac{\partial u}{\partial z} + \frac{\partial w}{\partial x} \right)^2 + \left(\frac{\partial v}{\partial z} + \frac{\partial w}{\partial y} \right)^2$$

There have been numerous refinements of the original Smagorinsky model but it is difficult to assess the improvements offered by these newer schemes. There are two reasons for this. First, the structure of the fire plume is dominated by the large scale resolvable eddies so that even a constant eddy viscosity gives results almost identical with those obtained with the Smagorinsky scheme [19]. Second, the lack of precision in most large scale fire data makes it difficult to sort out the subtleties associated with these models. For the time being, the Smagorinsky model with $C_s = 0.14$ produces satisfactory results for most large scale applications where boundary layers are not important.

The pressure perturbation is solved by taking the divergence of the momentum equation which results in an elliptic partial differential equation for $\mathcal{H}$

$$\nabla^2 \mathcal{H} = - \frac{\partial (\nabla \cdot \mathbf{u})}{\partial t} - \nabla \cdot \mathbf{F} \tag{8}$$

where the convective and diffusive terms have been incorporated in the term $\mathbf{F}$.

2.2. Combustion model

For the large eddy simulations, a sub-grid thermal element model (TEM) is formulated to represent the fire. A large number of Lagrangian particles are introduced into the plume, releasing heat as they are convected by the thermally induced motion [13, 14]. The combustion and hydrodynamics are coupled since the fluid motion determines where

the heat is released, while the heat release determines the motion. The concept is based on mixture-fraction theory for the transport of a conserved scalar that describes a reacting species. The TEM requires that the burning rate be prescribed as an input into the calculation. It is intended for applications where small scale mixing and diffusive processes that control non-premixed combustion cannot be resolved on the grid used to perform the simulation.

The overall heat release rate $\dot{q}$ from the fire is discretized as thermal elements that represent pyrolyzed fuel. At a specified surface, such as the fuel bed, thermal elements are ejected at a rate of $\dot{n}''$ particles per unit time per unit area with a small normal velocity into the flow domain. The heat release rate of a single thermal element is given by

$$\dot{q}_{p,j} = \frac{\dot{q}''}{\dot{n}''} \frac{1}{t_b} \qquad (t - t_0 < t_b)$$

where $\dot{q}''$ is the heat release rate per unit area of the fuel bed and t_b is the burn-out time of the thermal element. The burn-out time is obtained from the plume correlations of Baum and McCaffrey [17]. It is assumed that the thermal element burns out somewhere in the intermittent region of the plume, $1.32\,D^* < z < 3.30\,D^*$, where z is the height above the fire bed, $D^* = (\dot{q}/(\rho_0 c_p T_0 \sqrt{g}))^{2/5}$ is the characteristic diameter of the fire, and $\dot{q}$ is the total heat release rate of the fire. The burn-out time falls somewhere between $1.05\sqrt{D^*/g} < t_b < 1.86\sqrt{D^*/g}$ and is usually a few tenths of a second. The heat release term in (4) is the summation of convective heat release rates of the individual thermal elements in a grid cell of volume $\delta x \delta y \delta z$.

$$\dot{q}''' = \frac{\sum \dot{q}_{p,j}}{\delta x \delta y \delta z}$$

For the inclusion of oxygen transport in the calculation, the burn-out time of any thermal element will vary based on the concentration of oxygen in the surrounding gas. Oxygen is consumed in any given control volume based on the amount of heat generated in the control volume. The source term in the oxygen transport equation (2) becomes

$$\dot{W}_{O_2} = -\frac{\dot{q}'''}{\Delta H_{O_2}}$$

where ΔH_{O_2} is the amount of heat liberated per unit mass of oxygen consumed (usually about 13,100 kJ/kg O_2). When the oxygen mass fraction Y_{O_2} falls to a certain prescribed lower limit, combustion is assumed to stop, and the unburned fuel associated with the thermal elements remains unburned until more oxygen is available.

2.3. Numerical formulation

The equations numerically solved are the conservation of mass (1), species (2), momentum (3), and the Poisson equation for the total pressure which is formulated from

the energy equation (4) and state equation (5). The combustion is simulated via the thermal element model as described in section 2.2. The spatial derivatives are discretized with second-order central differencing, and a second-order explicit Runge-Kutta scheme is used to advance the velocity and temperature fields. The linear algebraic system arising from the discretization of the Poisson equation (8) has constant coefficients and can be solved to machine accuracy by direct (non-iterative) methods that utilize fast Fourier transforms and block tri-diagonal solvers. The grid is rectangular with uniform spacing in the horizontal directions and stretching in the vertical direction. The discretization for a computational cell is based on staggered-gridding techniques.

No-flux boundary conditions are specified by asserting that

$$\frac{\partial \mathcal{H}}{\partial n} = -F_n$$

at solid walls, where F_n is the normal component of $\mathbf{F}$ at the wall. Therefore, the normal component of velocity at the wall does not change with time, and indeed remains zero assuming the flow velocity is initially zero. At open external boundaries it is assumed that the perturbation pressure is zero. Thermal elements are ejected from the burner surface and burn according to the heat release rate per unit area $\dot{q}''$ which is specified as an input. An adiabatic boundary condition is used so that there is no temperature gradient normal to the burner surface. Refer to McGrattan et al. [13] for further details.

3. Large eddy simulations

The simulations of a whirling fire are based on the schematic shown in figure 1. The domain is a rectangular region with a square base 0.50 m per side and a 1.0 m height. A circular burner is centered at the base of the domain with diameter $d = 0.0863$ m and height $z_0 = 0.05$ m. The origin of the Cartesian coordinate system is centered at the base. The burner specifications represent a fuel source of acetone yielding a 14.4 kW fire. The oxygen transport model was used with a prescribed mass fraction burnout of 0.15.

Analogous to the experiments of Emmons and Ying [1], swirl can be induced by simulating an imposed circulation Γ_0 on the fire plume at a prescribed radial distance r_0 from the nominal centerline. Three dimensionless parameters govern the flow generated by this model:

(i) the heat-release rate $\dot{q}$ made dimensionless using thermal properties of the ideal gas

(ii) the circulation made dimensionless using a characteristic flame diameter D^* [17] and buoyant velocity $\sqrt{gD^*}$, where $\Omega/\alpha = (\Gamma_0/2\pi r_0^2)/\alpha$

(iii) a Reynolds number based on the buoyant velocity and flame diameter.

The parameter α is the reciprocal of a time scale which characterizes the flame strain due to buoyancy $\alpha = \sqrt{g/D^*}$. Therefore, the parameter Ω/α provides a measure of the effects of swirl-induced motion to buoyancy-driven motion. The Reynolds number is defined using characteristic parameters most relevant to the described problem. However, its definition should not be confused with the dynamic Reynolds number of the large scale simulations (refer to section 2.1). Additional dimensionless parameters are the ratio of length scales r_0/D^* and d/D^*; note that for these simulations the parameters are fixed and of order unity.

Results are presented for the large eddy simulations using a rectangular grid. Numerical tests were performed to determine the grid size necessary to resolve the flowfield with the best accuracy. Five mesh sizes ranging from 32^3 cells to 128^3 cells were used in the analysis. Based on *Richardson's extrapolation*, simulations calculated on a 72^3 grid (consisting of 373,248 cells) yields a relative error of about 4%. An average simulation takes approximately 18 μs per time step per cell on an SGI Octane/SI R10000 195MHz processor,‡ and requires about 12000 time steps for 20 s of simulation time.

The LES model was found to reproduce mean temperature and buoyant velocity correlations for large fire plumes in the absence of circulation over most of the simulated domain. Figures 2(a–b) compare the simulations with the McCaffrey correlations for the time-averaged centerline temperature and vertical velocity, respectively. Baum and McCaffrey [17] define three major zones for a typical fire plume. The zones are referred to as 1.) the continuous (visible) flame for $0 < (z - z_0)/D^* < 1.32$, 2.) the intermittent region for $1.32 \leq (z - z_0)/D^* \leq 3.30$, and 3.) the plume region for $3.30 < (z - z_0)/D^*$. Time-averaged radial temperature and velocity profiles have been shown previously by Baum, et al [19]. The good correspondence between the correlation data and the simulations is very encouraging, and provides confidence for the LES formulation.

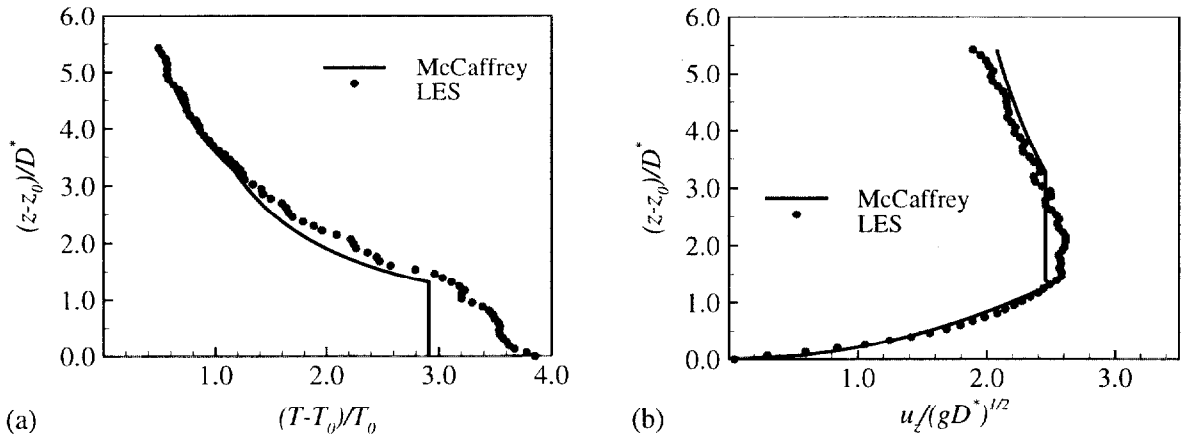

Figure 2. Comparison of the McCaffrey correlations [17] with LES for the time-averaged centerline a) temperature, and b) vertical velocity.

However, it is worthwhile to note that near the base of the fire the correspondence between the temperature correlations and LES deviates. The discrepancy is not a failure of the correlations but is a limitation of the current model. Neither the correlations nor the numerical model were constructed to apply near the base of a fire, but rather serve as a global description of flow dynamics. There is presently insufficient concensus between experiments to properly guide the formulation of a model to represent the entrainment region close to the fuel source [20]. The reason for this is two-fold: 1.) the region near the base of the fire is sensitive to the fuel geometry and can drastically change depending on the boundary conditions, experimental apparatus, etc., and 2.) there is great uncertainty in the measurements of entrainment rates near the fuel source due to localized effects.

The fire plume was simulated with an imposed circulation at a distance $r_0 = 0.2$ m measured from the nominal plume center and along the entire height of the domain. A comparison of the instantaneous temperature fields for a non-swirling ($\Omega/\alpha = 0.0$) and swirling fire ($\Omega/\alpha = 0.536$) is shown in figures 3(a–b), respectively. The non-swirling flame in figure 3(a) shows the onset of characteristic puffing associated with a typical fire [19, 21] as two hot regions near $z/D^* = 0.5$ and 1.0. However, the swirling fire (figure 3(b)) tends to have a continuous flame up to $z/D^* = 2.3$. Another difference is that the temperature contours shown in figure 3(b) define the continuous flame as being more tapered and constricted near the centerline than the non-swirling flame. Contours of heat release rate per unit volume $\dot{q}'''$ are shown in figure 4(a–b) for $\Omega/\alpha = 0.0$ and 0.536. Note that the swirling fire has more regions of high heat release rate than the non-swirling fire.

A three-dimensional representation of the two cases is shown in figures 5(a–b). The figures are isotherms for three temperature levels corresponding to the different plume regimes defined previously. Sample Lagrangian trajectories are shown as ribbons which follow the path of a streamline. The trajectory of figure 5(a) shows how a particle entrained in the non-swirling fire is drawn towards the center of the plume and then merely travels straight-up. A particle entrained in a swirling fire is also drawn towards the center of the plume but wraps around the plume a few times near the base of the fire before accelerating vertically. The general fluid motion of a swirling fire is unstable, as the fire typically oscillates or precesses within the boundaries of the fire bed. Bearing this in mind, time-averaged data is now presented.

The time-averaged temperature fields shown in figures 6(a–b) are not as elucidating as the instantaneous fire images (3(a–b)). The temperature contours of the non-swirling fire (3(a)) are more symmetric than the swirling fire (3(b)). It appears that time-averaging smears out the precessing motion of the swirling flows. However, to draw comparisons with experimental work, the remainder of this paper will consider results for the mean flowfields.

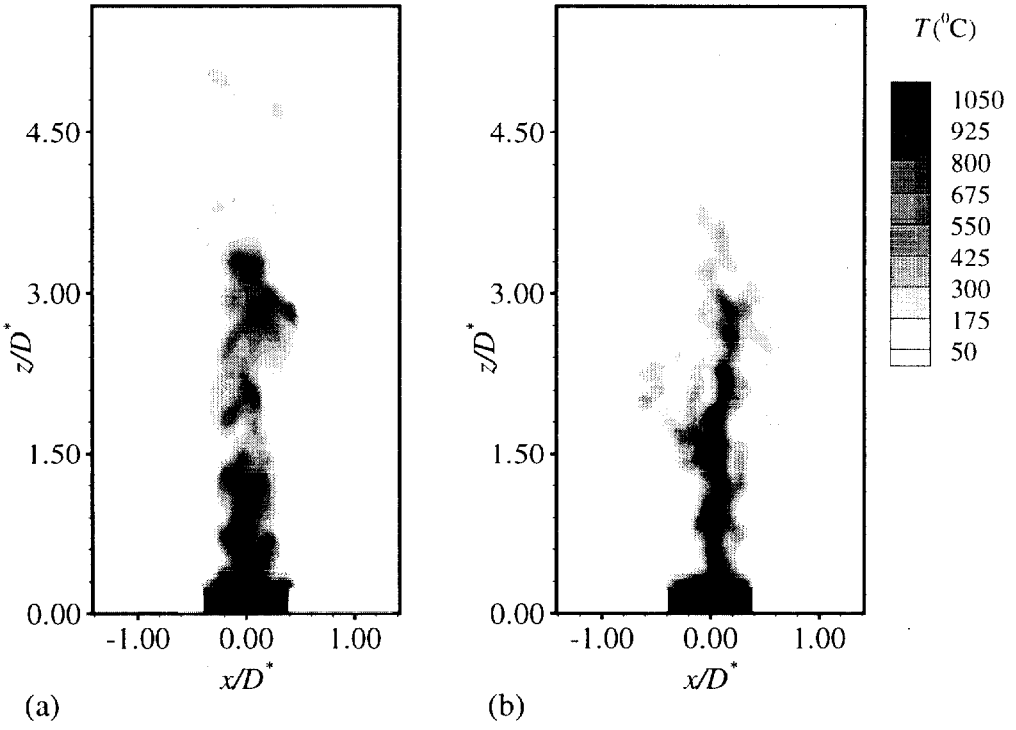

Figure 3. Instantaneous temperature field at the plume centerplane for a) non-swirling fire $\Omega/\alpha = 0.0$, and b) whirling fire $\Omega/\alpha = 0.536$.

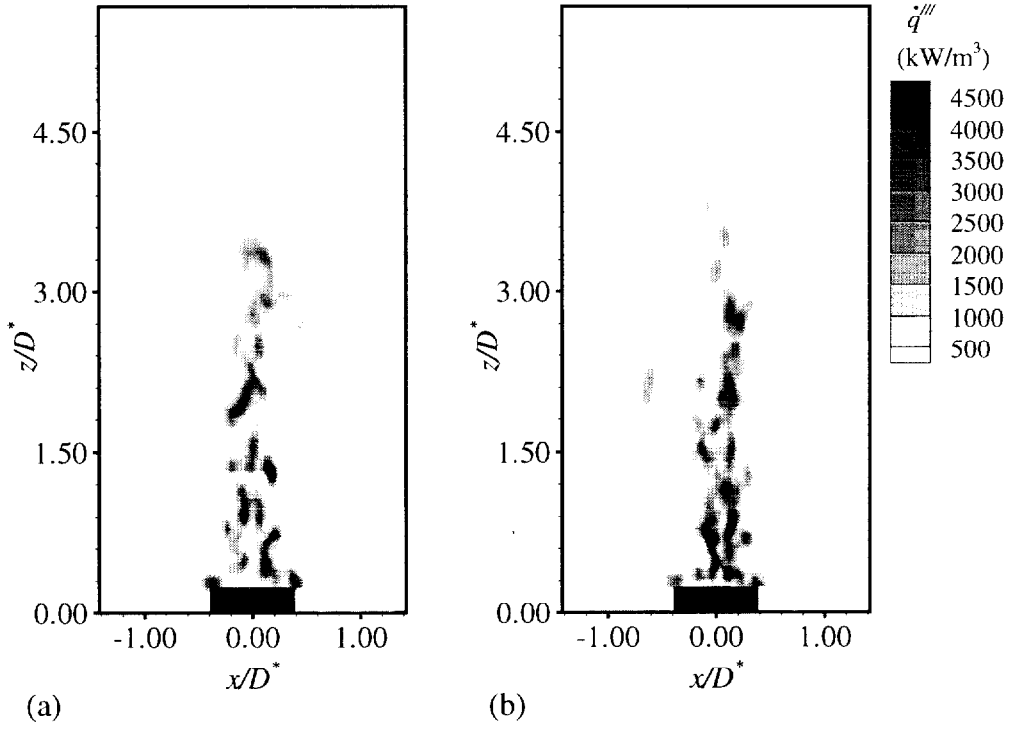

Figure 4. Instantaneous heat release rate per unit volume at the plume centerplane for a) non-swirling fire $\Omega/\alpha = 0.0$, and b) whirling fire $\Omega/\alpha = 0.536$.

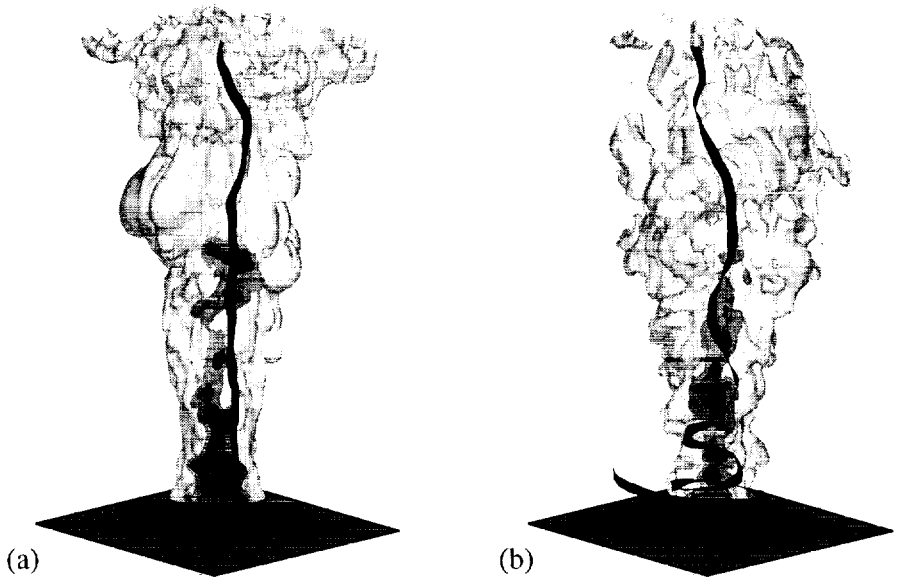

Figure 5. Simulations of a plume for a) non-swirling fire $\Omega/\alpha = 0.0$, b) whirling fire $\Omega/\alpha = 0.536$. Isotherms are shown for three major zones: the continuous flame (dark gray), the intermittent region (medium gray), and the plume region (light gray). The black ribbons are sample Lagrangian trajectories of the flowfields.

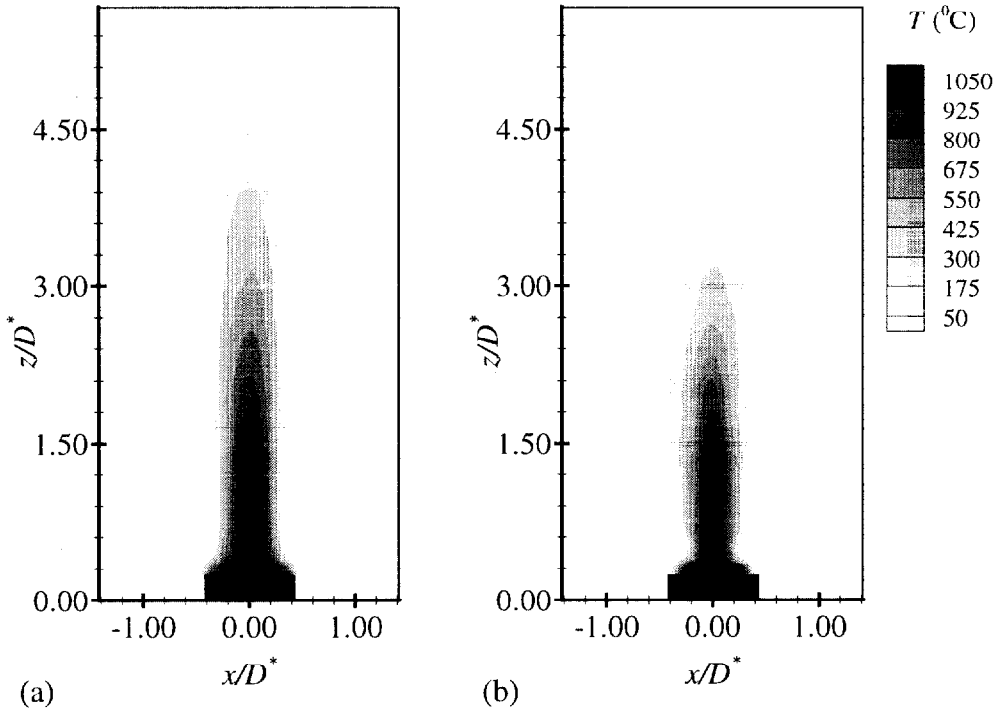

Figure 6. Time-averaged temperature fields at the plume centerplane for a) non-swirling fire $\Omega/\alpha = 0.0$, and b) whirling fire $\Omega/\alpha = 0.536$.

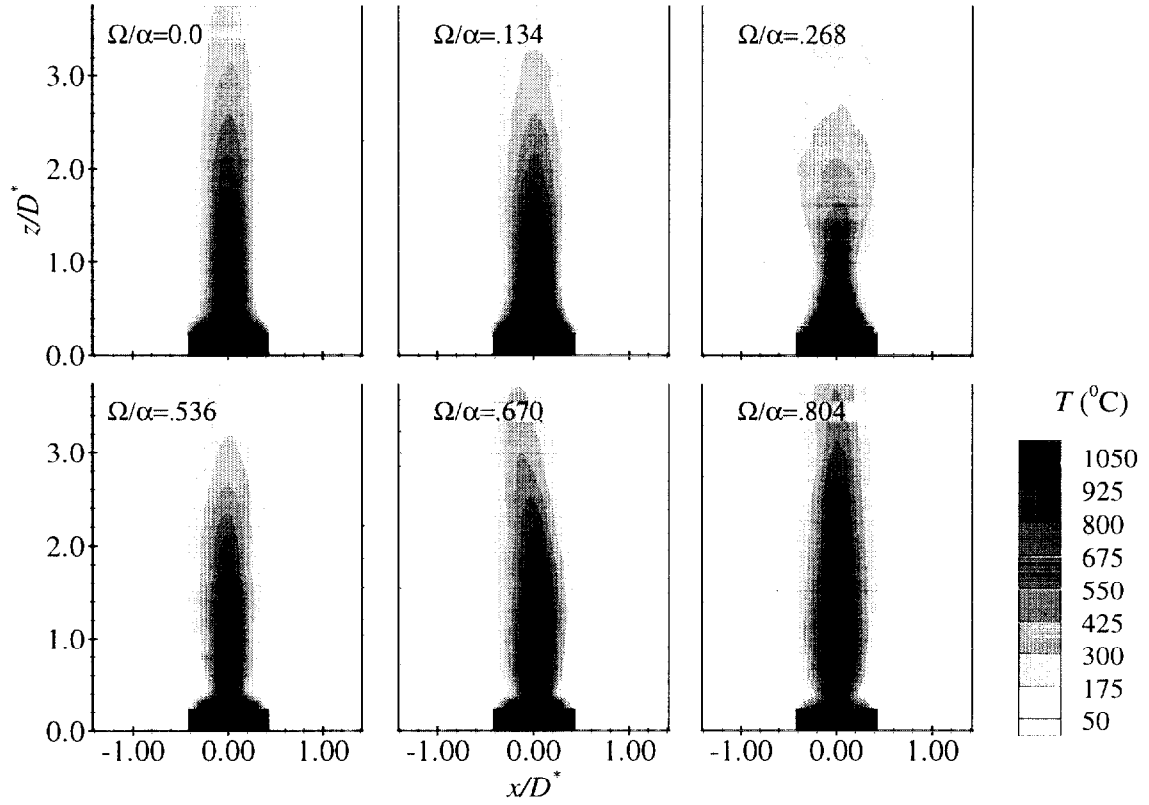

Figure 7. Time-averaged temperature fields at the plume centerplane for varying circulation Ω/α.

Figure 7 shows six cases of the time-averaged temperature fields for values of circulation from $\Omega/\alpha = 0.0$ to $\Omega/\alpha \sim 0.8$. At first, increasing the circulation results in a larger region of high temperatures near the fire bed. The simulations then predict that further increasing the circulation above $\Omega/\alpha > .268$ reduces the region of high temperatures. However, the isotherms near the central region of the plume show that the flame has narrowed and stretched vertically for $\Omega/\alpha \geq 0.536$. The flame-lengthening trends discussed by Chigier et al. [9] are qualitatively similar to that reported here. Furthermore, there is very good agreement when cases $\Omega/\alpha = 0.0$ and 0.804 (figure 7) are compared with the temperature distributions of the propane diffusion flame [9], for both flame shape and temperature ranges.

Another way to interpret the varying effects of circulation is shown as contours of time-averaged heat release rate per unit volume in figure 8. Increasing the circulation reduces the overall volume of the fire plume and increases the region of high heat release rates within the central region of the flame. The heat release rate contours near the base for $\Omega/\alpha > 0.50$ have two peaks and a small dip near the centerline, which seems to be a consequence of time-averaging an oscillating flow. The experimental observations

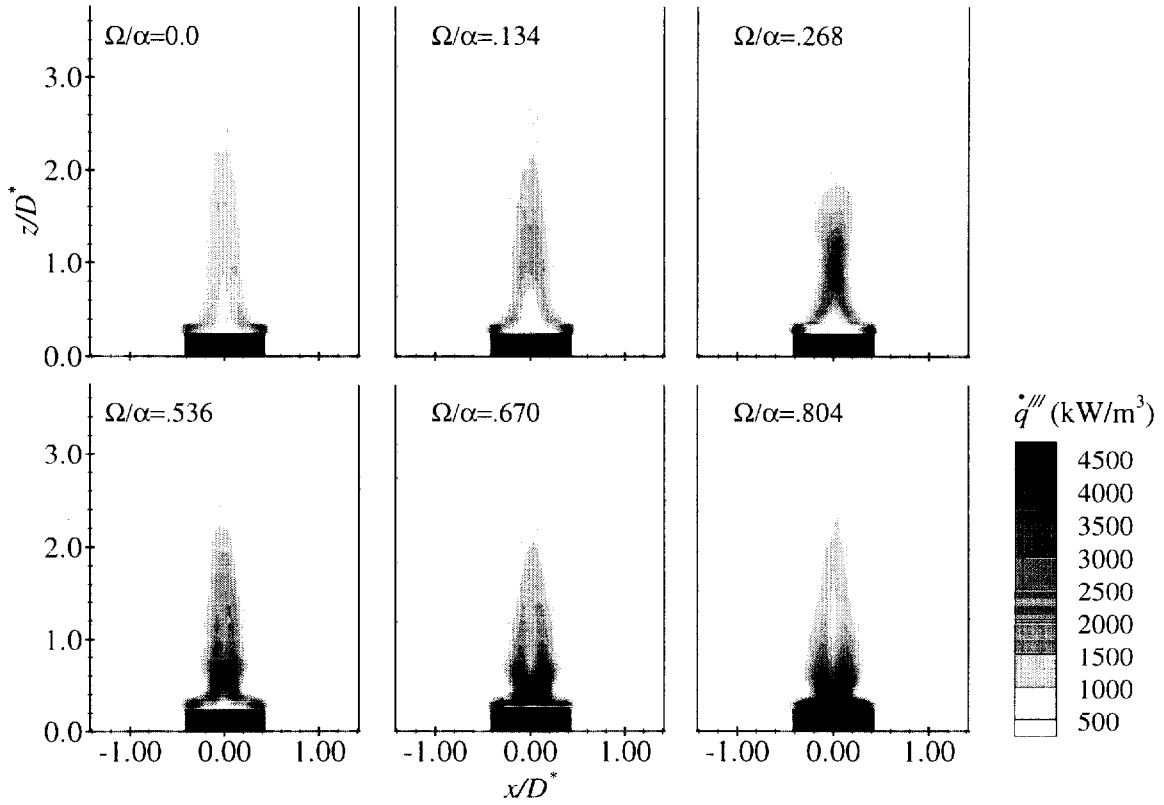

Figure 8. Time-averaged heat release rate per unit volume at the plume centerplane for varying circulation Ω/α.

of Emmons and Ying [1] indicate that the heat release rate is significantly increased by the swirling motion. Although the numerical methodology described in section 2 does not model varying heat release rate, it is very encouraging that the simulated results show larger regions of higher heat release rates.

Time-averaged temperature profiles for the six cases of circulation are shown in figure 9 at $(z - z_0)/D^* = 1.5$. Overall, the temperature profiles have nearly the same distribution along x at the centerplane. A closer examination of the temperatures near the centerline ($x = 0.0$) reveals an interesting pattern. Initially, the mean temperature at the centerline reduces with increasing circulation up to $\Omega/\alpha = 0.536$. Further increasing circulation then results in an increase of the mean temperature at the centerline. The decreasing/increasing temperature trends are also reflected in figure 7 of time-averaged isotherms.

At this point we explore the possibility of defining a characteristic flame height for the six cases presented. According to analyses of Orloff and deRis [22], the size and shape of pool fires can be constructed through Froude modeling. Their model was substantiated with experimental data from pool fires of various fuels. The luminous

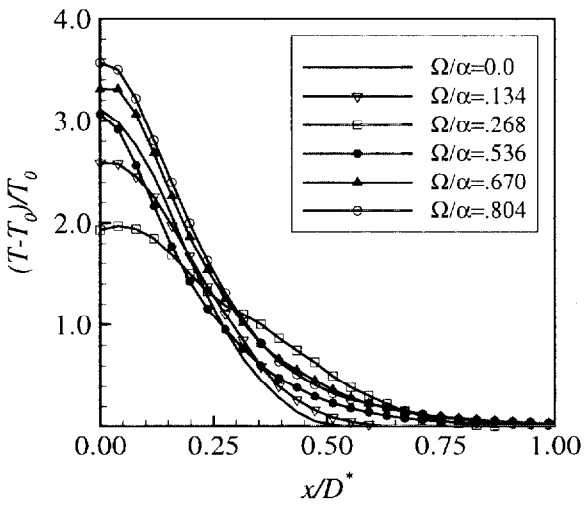

Figure 9

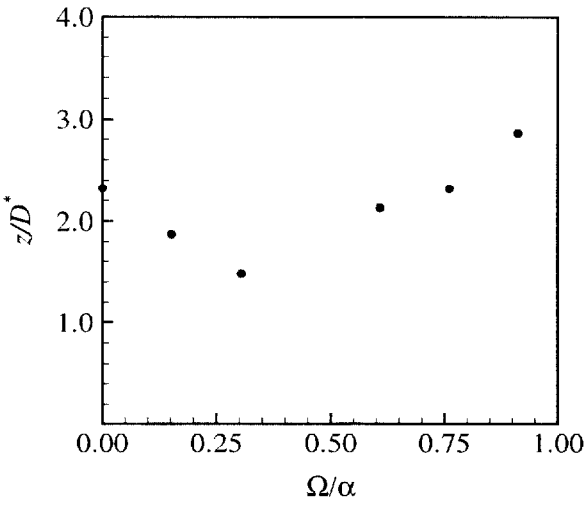

Figure 10

Figure 9. Mean temperature profiles at $(z - z_0)/D^* = 1.5$ for varying circulation.

Figure 10. Mean centerline flame height (based on 925°C) versus circulation.

flame volume was defined by an effective flame temperature of 1200 K (independent of fuel) for which the Froude modeling suggested an average volumetric heat release rate of 1200 kW/m^3. Returning to figure 7, the flame height can be visualized as the contour marking 925°C. Likewise, figure 8 deliniates the flame shape between contours 1000-1500 kW/m^3. A characteristic mean flame height at the centerline based on 925°C is shown in figure 10 to re-emphasize the decreasing/increasing flame height trends previously discussed.

The numerical simulations can be compared to the experimental findings of Emmons and Ying [1]. Their study of a fire whirl included temperature profiles for different values of circulation. The experimental trends indicate that with increasing circulation, the maximum mean temperature peaked off-center. Figures 11(a–b) are mean temperature profiles for $\Omega/\alpha = 0.0$ and 0.536. The maximum mean temperature for the non-swirling fire always occurs at the plume nominal centerline and decreases with height. In the case of the swirling fire, the maximum temperatures also occurred at the nominal centerline. Further data analyses indicated that depending on the number of realizations captured in one complete revolution of the fire, the time-averaged data may yield asymmetric features of the flow. It is not clear if the off-centerline peak temperatures as reported in [1] are an artifact of the oscillating motion of the fire or due to the location of the flame sheet.

The swirl velocity profiles provide further information regarding the fluid motion. The time-averaged profiles are shown in figure 12 for varying circulation at position

$(z-z_0)/D^* = 1.5$. In the absence of circulation, the mean swirl velocity is approximately zero with some fluctuation near the plume centerline and closest to the fire bed. Once circulation is introduced, the magnitude of the swirl velocity increases with increasing circulation. Peak values of swirl velocity occur at $x/D^* \sim 0.4$ which corresponds to the edge of the burner and may be indicative of high heat release rates near the edge of the flame. Beyond $x/D^* = 1.1$, the position at which circulation is imposed, the swirl velocity decays to zero. Figure 13 is a plot of the mean swirl velocity versus x/D^* at various heights for $\Omega/\alpha = 0.536$. The curves indicate that the peak swirl velocity decreases with increasing height z. As the plume spreads radially, the swirl velocities tend to mix outward and reduce the swirl velocities, suggesting that buoyancy increasingly dominates the dynamics farther up the plume.

4. Concluding remarks

Numerical simulations of fire plumes were conducted in order to ascertain the dynamic attributes of swirl and buoyancy in whirling fires. The LES methodology for simulating fires is based on direct solution of the large scales and sub-grid scale approximations for the dynamic viscosity and heat release. The simulations for non-swirling fires are in very good agreement with mean temperature and buoyant velocity correlations for large fires. The approach taken for swirling fires was to impose circulation while maintaining a constant heat release rate.

It was shown that increasing circulation has a strong influence on the shape of the fire plume. The whirling fires increased in length and constricted radially, consistent with previously published literature. The temperature trends along the centerline decreased then increased in values for increasing circulation. Despite the fixed heat release, increasing circulation increased the region of maximum heat release rates while reducing the overall volume of the fire. The swirl velocities also increased with increasing swirl. In addition, it was determined that farther up the plume buoyancy effects are more dominant than the swirl velocities.

The present study carefully explored the effects of circulation on a fire plume. The scenario of a fixed fire strength and variable circulation was the first numerical study to systematically analyze the relationship between swirl and buoyancy. A set of well-defined experiments to match the current numerical approach will be beneficial for a more quantitative comparison and validation. The next step will be to relax the condition of a fixed heat release to one that varies according to the radiation heat feedback to the surface of the fire. This, in itself, changes the current problem of an imposed fuel flow to a pool fire.

‡ The computer is identified to specify the computational timings and is not intended to imply recommendation nor endorsement by NIST.

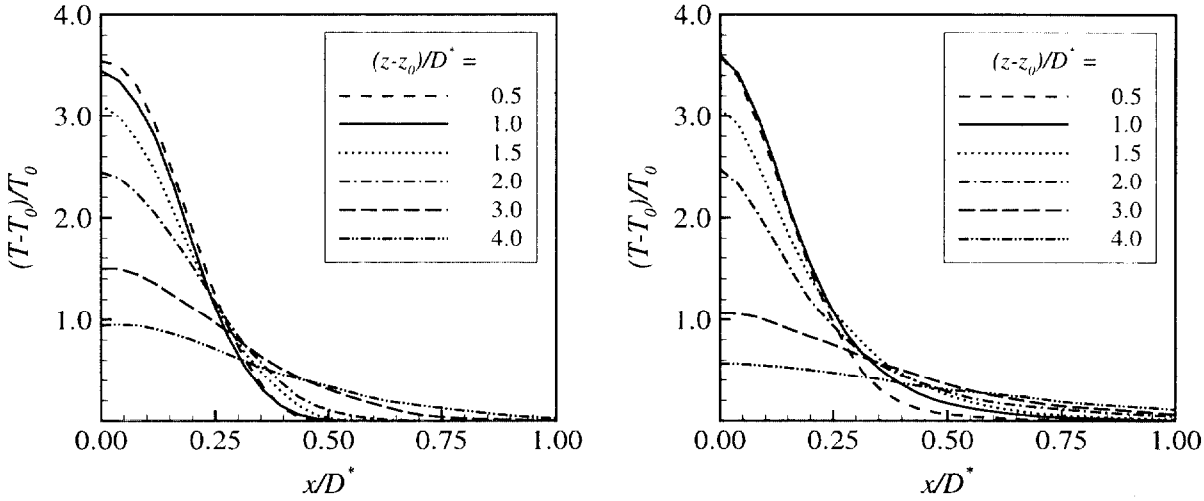

(a) (b)

Figure 11. Time-averaged temperature profiles for a) non-swirling fire $\Omega/\alpha = 0.0$ and b) whirling fire $\Omega/\alpha = 0.536$, for varying height $(z - z_0)/D^*$.

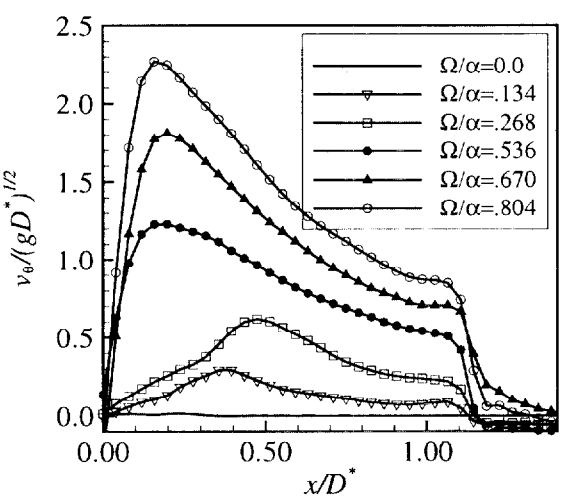

Figure 12

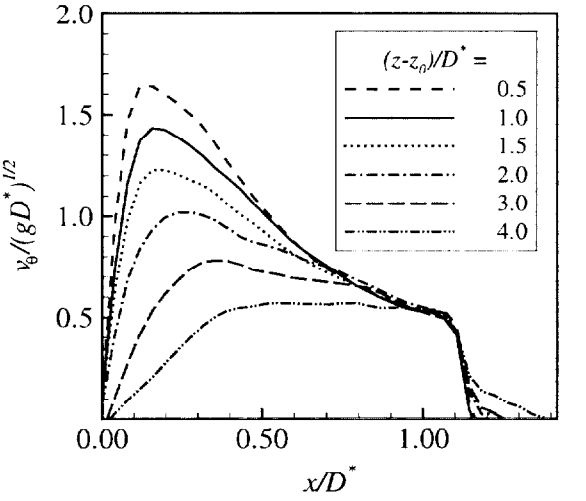

Figure 13

Figure 12. Mean swirl velocity profiles at $(z - z_0)/D^* = 1.5$ for varying circulation.

Figure 13. Mean swirl velocity profiles of whirling fire $\Omega/\alpha = 0.536$ for varying height.

5. Acknowledgments

This research was supported by a National Research Council Postdoctoral Fellowship. The first author is grateful for helpful discussions with Dr. William (Ruddy) Mell during the course of this research. This manuscript is dedicated to the pioneering work of Professor H.W. Emmons (1912–1998).

References

[1] Emmons, H.W. and S.-J., Ying, The Fire Whirl, *Eleventh Symposium (International) on Combustion*, pp. 475–488 (1967).

[2] Morton, B.R., The Physics of Fire Whirls, *Fire Research Abstracts and Reviews*, **12**(1):1–19 (1970).

[3] Thomas, T.G. and Takhar, H.S., Swirling Motion in a Buoyant Plume, *Acta Mechanica*, **71**:185–193 (1988).

[4] Williams, F.A., Urban and Wildland Fire Phenomenology, *Progress in Energy and Combustion Science*, **8**:317–354 (1982).

[5] Soma, S. and Saito, K., Reconstruction of Fire Whirls Using Scale Models, *Combustion and Flame*, **86**:269–284 (1991).

[6] Hirano, T. and Saito, K., Fire spread phenomena: The role of observation in experiment, *Progress in Energy and Combustion Science*, **20**:461–485 (1994).

[7] Satoh, K. and Yang, K.T., Experimental Observations of Swirling Fires, *ASME HTD*, **335**:393–400 (1996).

[8] Satoh, K. and Yang, K.T., Simulations of Swirling Fires Controlled by Channeled Self-generated Entrainment Flows, *Fire Safety Science – Proceedings of the Fifth International Symposium*, pp. 201–212 (1997).

[9] Chigier, N.A., Beér, J.M., Grecov, D., and Bassindale, K., Jet Flames in Rotating Flow Fields, *Combustion and Flame*, **14**:171–180 (1970).

[10] Tangirala, V. and Driscoll, J.F., Temperature within Non-premixed Flames: Effects of Rapid Mixing Due to Swirl, *Combustion, Science and Technology*, **60**:143–162 (1988).

[11] Gabler, H.C., Yetter, R., and Glassman, I., Asymmetric Whirl Combustion: A New Approach for Non-Premixed Low NOx Gas Turbine Combustor Design, *Proceedings of the 34th AIAA/ASME/SAE/ASEE Joint Propulsion Conference*, AIAA Paper 98-3530, Cleveland, OH, July 1998.

[12] Rehm, R.G. and Baum, H.R., The equations of motion for thermally driven, buoyant flows, *Journal of Research, National Bureau of Standards*, **83**(3):297–308 (1978).

[13] McGrattan, K.B., Baum, H.R., and Rehm, R.G., Large Eddy Simulations of Smoke Movement, *Fire Safety Journal*, **30**(2):161–178 (1998).

[14] Baum, H.R., Ezekoye, O.A., McGrattan, K.B., and Rehm, R.G., Mathematical modeling and computer simulation of fire phenomena, *Theoretical and Computational Fluid Dynamics*, **6**(2–3):125–139 (1994).

[15] Mell, W.E., McGrattan, K.B., and Baum, H.R., Numerical simulation of combustion in fire plumes, *Twenty-Sixth Symposium (International) on Combustion*, pp. 1–14 (1996).

[16] McCaffrey, B.J., Purely Buoyant Diffusion Flames: Some Experimental Results, *National Bureau of Standards Report*, (1979).

[17] Baum, H.R. and McCaffrey, B.J., Fire Induced Flow Field - Theory and Experiment, *Fire Safety Science - Proceedings of the Second International Symposium*, pp. 129–148 (1989).

[18] Smagorinsky, J., General circulation experiments with the primitive equations. I. The basic experiment, *Monthly Weather Review*, **91**:99 164 (1963).

[19] Baum, H.R., McGrattan, K.B., and Rehm, R.G., Three Dimensional Simulation of Fire Plume Dynamics, *Fire Safety Science – Proceedings of the Fifth International Symposium*, pp. 511–522 (1997).

[20] Zhou, X.C., Gore, J.P., and Baum, H.R., Measurements and prediction of air entrainment rates of pool fires, *Twenty-Sixth Symposium (International) on Combustion*, pp. 1453–1459 (1996).

[21] Cetegen, B.M. and Ahmed, T.A., Experiments on the Periodic Instability of Buoyant Plumes and Pool Fires, *Combustion and Flame*, **93**:157–184 (1993).

[22] Orloff, L. and de Ris, J., Froude Modeling of Pool Fires, *Nineteenth Symposium (International) on Combustion*, pp. 885–895 (1982).

NIST-114 (REV. 6-93) ADMAN 4.09

U.S. DEPARTMENT OF COMMERCE
NATIONAL INSTITUTE OF STANDARDS AND TECHNOLOGY

MANUSCRIPT REVIEW AND APPROVAL

(ERB USE ONLY)	
ERB CONTROL NUMBER: G	DIVISION:
PUBLICATIONS REPORT NUMBER: No. NISTIR 6341	CATEGORY CODE:
PUBLICATION DATE: July 1999	NO. PRINTED PAGES:

INSTRUCTIONS: ATTACH ORIGINAL OF THIS FORM TO ONE (1) COPY OF MANUSCRIPT AND SEND TO: WERB SECRETARY, BUILDING 820, ROOM 125

TITLE AND SUBTITLE (CITE IN FULL)

Simulating Fire Whirls

CONTRACT OR GRANT NUMBER

TYPE OF REPORT AND/OR PERIOD COVERED
NISTIR

AUTHOR(S) (LAST NAME, FIRST INITIAL, SECOND INITIAL)

Battaglia, F., McGrattan, K.B., Rehm, R.G. and Baum, H.R.

PERFORMING ORGANIZATION (CHECK (X) ONE BOX)

- [X] NIST/GAITHERSBURG
- [ ] NIST/BOULDER
- [ ] NIST/JILA

LABORATORY AND DIVISION NAMES (FIRST NIST AUTHOR ONLY)
BFRL/Fire Safety Engineering Division

SPONSORING ORGANIZATION NAME AND COMPLETE ADDRESS (STREET, CITY, STATE, ZIP)

PROPOSED FOR NIST PUBLICATION

- [ ] JOURNAL OF RESEARCH (NIST JRES)
- [ ] J. PHYS. & CHEM. REF. DATA (JPCRD)
- [ ] HANDBOOK (NIST HB)
- [ ] SPECIAL PUBLICATION (NIST SP)
- [ ] TECHNICAL NOTE (TN)
- [ ] MONOGRAPH (NIST MN)
- [ ] NATL. STD. REF. DATA SERIES (NIST NSRDS)
- [ ] FEDERAL INFO. PROCESS. STDS. (NIST FIPS)
- [ ] LIST OF PUBLICATIONS (NIST LP)
- [X] INTERAGENCY/INTERNAL REPORT (NISTIR)
- [ ] LETTER CIRCULAR
- [ ] BUILDING SCI. SERIES
- [ ] PRODUCT STANDARDS
- [ ] OTHER
- [ ] —

PROPOSED FOR NON-NIST PUBLICATION (CITE FULLY): [ ] —U.S. FOREIGN— [ ]

PUBLISHING MEDIUM:	X	PAPER		DISKETTE		CD-ROM		WWW		OTHER

SUPPLEMENTARY NOTES

ABSTRACT (A 2000-CHARACTER OR LESS FACTUAL SUMMARY OF MOST SIGNIFICANT INFORMATION. IF DOCUMENT INCLUDES A SIGNIFICANT BIBLIOGRAPHY OR LITERATURE SURVEY, CITE IT HERE. SPELL OUT ACRONYMS ON FIRST REFERENCE.) (CONTINUE ON SEPARATE PAGE, IF NECESSARY.)

A numerical investigation of swirling fire plumes is pursued to understand how swirl alters the plume dynamics and combustion. One example is the "fire whirl" which is known to arise naturally during forest fires. This buoyancy-driven fire plume entrains ambient fluid as heated gases rise. Vorticity associated with a mechanism such as wind shear can be concentrated by the fire creating a vortex core along the axis of the plume. The result is a whirling fire. The current approach considers the relationship between buoyancy and swirl using a configuration based on fixing the heat release rate of the fire and imposing circulation. Large eddy methodologies are used in the numerical analyses. Results indicate that the structure of the fire plume is significantly altered when angular momentum is imparted to the ambient fluid. The vertical acceleration induced by buoyancy generates strain fields which stretch out the flames as they wrap around the nominal plume centerline. The whirling fire constricts radially and stretches the plume vertically.

KEY WORDS (MAXIMUM OF 9; 28 CHARACTERS AND SPACES EACH; SEPARATE WITH SEMICOLONS; ALPHABETIC ORDER; CAPITALIZE ONLY PROPER NAMES)
Flame whirls; plumes; circulation; buoyancy

AVAILABILITY:

- [X] UNLIMITED
- [ ] FOR OFFICIAL DISTRIBUTION - DO NOT RELEASE TO NTIS
- [ ] ORDER FROM SUPERINTENDENT OF DOCUMENTS, U.S. GPO, WASHINGTON, DC 20402
- [X] ORDER FROM NTIS, SPRINGFIELD, VA 22161

NOTE TO AUTHOR(S): IF YOU DO NOT WISH THIS MANUSCRIPT ANNOUNCED BEFORE PUBLICATION, PLEASE CHECK HERE. [ ]